Journal of Molecular Graphics and Modelling 74 (2017) 241–250

Contents lists available at ScienceDirect

Journal of Molecular Graphics and Modelling

journal homepage: www.elsevier.com/locate/JMGM

Topical Perspectives

# Molecular dynamics simulation of gas-phase ozone reactions with sabinene and benzene

H.F. Ridgway[a], B. Mohan[b], X. Cui[b], K.J. Chua[b,c,*], M.R. Islam[b,c]

[a] AquaMem Scientific Consultants, Rodeo, NM, USA
[b] Department of Mechanical Engineering, National University of Singapore, 9 Engineering Drive 1, Singapore 117576, Singapore
[c] Engineering Science Programme, National University of Singapore, 9 Engineering Drive 1, Singapore 117575, Singapore

ARTICLE INFO

*Article history:*
Received 5 January 2017
Received in revised form 15 April 2017
Accepted 18 April 2017
Available online 20 April 2017

*Keywords:*
Volatile organic compounds (VOCs)
Ozonation
Molecular mechanics
Formaldehyde
Sabina-ketone

ABSTRACT

Gas-phase reactions of ozone ($O_3$) with volatile organic compounds were investigated both by experiment and molecular simulations. From our experiments, it was found ozone readily reacts with VOC pure components and reduces it effectively. By introducing ozone intermittently, the reaction between VOC and ozone is markedly enhanced. In order to understand the relationship between intermediate reactions and end products, ozone reaction with benzene and alicyclic monoterpene sabinene were simulated via a novel hybrid quantum mechanical/molecular mechanics (QM/MM) algorithm that forced repeated bimolecular collisions. Molecular orbital (MO) rearrangements (manifested as bond dissociation or formation), resulting from the collisions, were computed by semi-empirical unrestricted Hartree-Fock methods (e.g., RM1). A minimum of 975 collisions between ozone and targeted organic species were performed to generate a distribution of reaction products. Results indicated that benzene and sabinene reacted with ozone to produce a range of stable products and intermediates, including carbocations, ring-scission products, as well as peroxy ($HO_2$ and $HO_3$) and hydroxyl (OH) radicals. Among the stable sabinene products observed included formaldehyde and sabina-ketone, which have been experimentally demonstrated in gas-phase ozonation reactions. Among the benzene ozonation products detected composed of oxygen mono-substituted aromatic $C_6H_5O$, which may undergo further transformation or rearrangement to phenol, benzene oxide or 2,4-cyclohexadienone; a phenomenon which has been experimentally observed in vapor-phase photocatalytic ozonation reactions.



## 1. Introduction

Volatile organic compounds (VOCs) causes many health issues related to Indoor Air Quality (IAQ) [1–3]. Indoor air quality improvement has been instituted by various organizations based on the concentration levels of different pollutants [4–6]. Treatment of indoor air not only helps to improve the living standards of people but also reaps energy savings by reducing the amount of outdoor air intake [7,8]. Though the presence of VOCs in indoor air has various adverse health effects and is the primary reason for sick building syndrome, there are only few abatement technologies currently available. The VOCs abatement techniques can be broadly classified into two categories, namely (a) Destruction of VOCs which includes techniques like oxidation and bio-filtration, and (b) Recovery of VOCs which includes absorption, adsorption, condensation and membrane separation [9]. Each of the methods has its own advantages and limitations. Thermal oxidation is the most commonly used method, however it suffers from the production of harmful combustion products which require further treatments. The adsorption technique requires high capital and operating cost to separate the VOCs from the desorbed solution. Though the process of condensation is quite simple, nevertheless it is expensive to operate due to the high boiling range of VOCs and the associated extreme operating pressure and temperature. In addition, the absorption technique requires a knowledge database on vapor-liquid equilibriums of different VOCs in order to design a proper equipment for the processing. Bio-filtration technique suffers from selective VOC destruction i.e. it requires selective micro-organisms to capture specific VOC and is sensitive towards starvation when it is not exposed to VOC [10]. One of the prominent techniques in abatement of VOCs is by gas phase ozonation reaction [11,12]. Ozone, being a very strong oxidizing agent, is capable of oxidizing numerous gas and aqueous phase species including various types of VOCs. Ozone, by itself (or in combination with porous and/or catalytic adsorbents) has been extensively employed for the destructive decomposition of naturally-occurring and anthropogenic pollutants in air and water [12–15]. In this study, the

* Corresponding author at: Department of Mechanical Engineering, National university of Singapore, 9 Engineering Drive 1, Singapore 117576, Singapore.
*E-mail address:* mpeckje@nus.edu.sg (K.J. Chua).

http://dx.doi.org/10.1016/j.jmgm.2017.04.020
1093-3263/

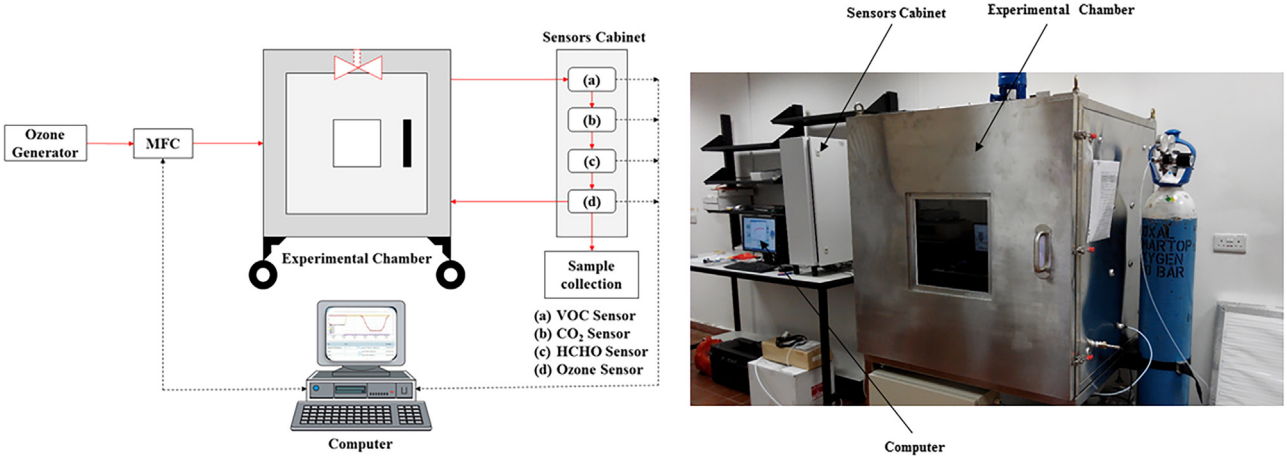


**Fig. 1.** Experimental setup for studying and monitoring VOC ozonation.

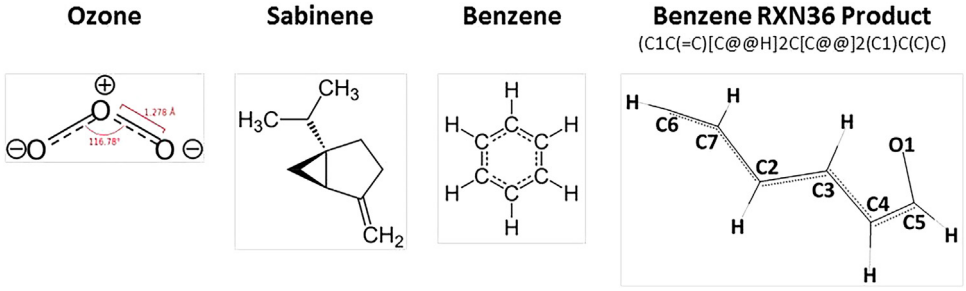


**Fig. 2.** Compounds modeled in this study and used in the SFMD reaction simulations.

treatment of pure VOC chemicals viz, Acetone, Ethylbenzene and xylene with ozone were first studied experimentally. The objective of this study is to demonstrate that ozone has the capability to abate a variety of gas-phase volatile organic compounds (VOCs). It has been reported that reaction between ozone and VOC leads to the formation of a number of intermediate compounds such as aldehydes, ketones and organic acids [16]. Due to a deficiency of existing information regarding specific intermediates and stable end products, molecular dynamic (MD) simulations were concurrently carried out in this work with the aim of predicting the potential ozonation reaction outcomes using both benzene and monoterpene sabinene as target compounds. The MD simulations combined elements of bimolecular collision theory and molecular orbital (MO) calculations to generate early (i.e., first or second generation) putative reaction products.

## 2. Methodology

### 2.1. Experimental setup

An experimental setup has been developed and established to study the effect of ozone on VOCs abatement as shown in Fig. 1. The experimental setup comprised of an insulated chamber of size 1 m × 1 m × 1 m fitted with a fan with variable speed control for proper mixing of air inside the chamber. Ozone was introduced to the chamber through a precise mass flow controller. It was produced using an ozone generator supplied with 99.95% pure oxygen. Sensors for measuring VOC, Ozone, Formaldehyde and $CO_2$ were provided to measure the concentration of various gases. The specifications of various sensors are given in Table 1.

The experiments were carried out with Acetone, Ethylbenzene and Xylene. First, the samples were introduced to the chamber for VOC emissions. The samples were removed from the chamber and the VOC concentration was monitored through the VOC sensor. Once the concentration of VOC reached steady conditions inside the chamber, a specific quantity of ozone is introduced to the chamber through the precise mass flow controller. The ozone generator is then switched off once desired ozone concentration was attained. The reaction between ozone and VOC was closely monitored and recorded through the sensors. Data were analyzed to evaluate the impact of the reactive ozone on VOC and their respective degradation rates.

### 2.2. Reaction simulations

Reactions that were modeled in this study included: (1) ozone + sabinene; (2) ozone + benzene; and (3) ozone + a linear ($C_6H_6O$) open-ring first-generation benzene transformation product (Fig. 2). Reactant species (ozone and target organics) were modeled using a combination of Classical mechanics and quantum mechanical (QM) methods. Briefly, ozone, benzene and sabinene models were prepared using the Newtonian MM+ and AMBER99 force fields provided in Hyperchem (Version 8.0.10; Hypercube, Inc., Gainsville, Florida, USA), followed by structure refinement and assignment of partial atomic charges by unrestricted Hartree-Fock (UHF) calculations using the RM1 semi-empirical method [17] and/or ab initio calculations using the 6-31G** polarization basis set. As shown in Figs. 2 and 3, this general approach resulted in reasonable molecular geometries for these compounds. The specific properties of ozone calculated using the RM1 (UHF) method are summarized in Fig. 3 and closely approximate experimentally-derived values.[1]

[1] http://cccbdb.nist.gov/exp2.asp?casno=10028156 for a summary of ozone physical and molecular properties.

**Table 1**
Specifications of the sensors.

| Sensor | Measurement ranges | Accuracy |
|---|---|---|
| VOC sensor | 0.1 to 1000 ppm | ±2% of reading |
| Ozone sensor | 0 to 10 ppm | ±(0.01 ppm + 7.5% of reading) |
| $CO_2$ sensor | 0 to 2000 ppm | ±(1.5% of range + 2% of reading) |
| Formaldehyde sensor | 0 to 10 ppm | ±0.1 ppm |

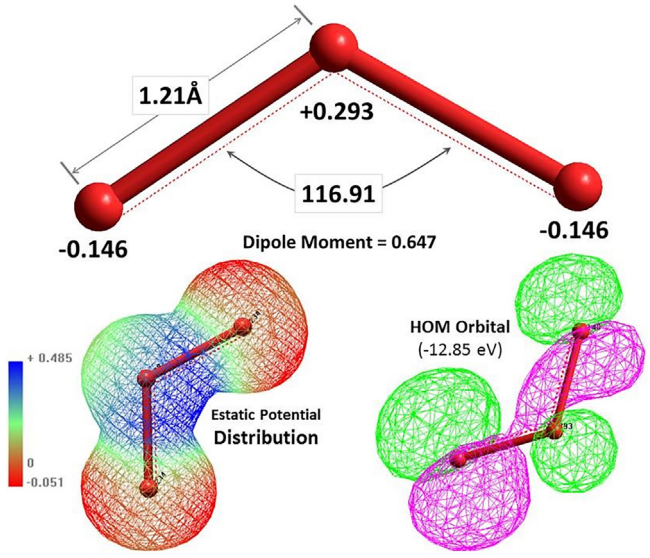


**Fig. 3.** Ozone properties calculated by the RM1 semi-empirical method (UHF).

The reaction simulation algorithm employed in this project is outlined in Fig. 4. It is referred to as the "Stepped Forced Molecular Dynamics" (SFMD) method since it affords the ability to force collisions between reacting species according to a special step function in which the overall MD trajectory is divided into a series of discrete QM steps ("QM runs") alternated with molecular mechanics (MM) optimization of the solvent (water) phase. Following each QM run, the solvent phase is energy minimized and allowed to re-adapt to the updated nuclear positions of the reactants. During QM cycles, the solvent system is "frozen" and represented as a perturbation on the one-electron Hamiltonian. In the present study, the step function was not invoked since no solvent was present in the molecular systems, with the exception of a single "ghost" water molecule (with mass and charge = 0) needed for the SFMD algorithm to function properly; i.e., all reactions were carried out in the gas phase (i.e., in vacuo). During the QM runs, the molecular orbitals (MOs) of the reacting species are computed using a suitable semi-empirical one-electron method, such as RM1 [17]. The SFMD time step for the QM runs was 0.001 ps and the total reaction time was 0.6 ps. In this study, a total reaction time of 0.60 ps was used, which was comprised of 600 independent MO calculations. A collision velocity of 75 Å/ps was used in all SFMD simulations. In a second part of the SFMD algorithm, both bond breakage and formation are computed by comparing final (i.e., post-reaction) bond lengths with a library of ideal (ground-state) bond lengths for all atom pairs and types in the system. Following "re-bonding" of the molecular system, the reaction products were scanned for their charge, mass, elemental composition and other molecular properties. For each reaction series, a frequency histogram of products is generated, which are categorized according to whether the parent (target) compound has undergone ring opening, hydrogen abstraction, electrophilic substitution/elimination, or other types of transformations. In some reaction series, the products were scanned for a specific reaction outcome, e.g., formation of formaldehyde or a particular ketone (e.g., sabina-ketone). The occurrence frequency of electrophilic attack on specific atom centers in the target compound was also monitored, as was the system potential energy and other MD parameters.

## 3. Results & discussion

### 3.1. VOC-ozone experimental outcome

There are over 100 VOCs present in the VOC emitting building materials like paints, glue, protective coatings etc. Among them, some of the main VOCs were tested inside the specially built environmental chamber to elucidate the reacting effects of ozone on pure VOCs. The pure VOCs that were tested include Acetone, Ethylbenzene and Xylene. Fig. 5 shows the impact of ozone on VOC. The

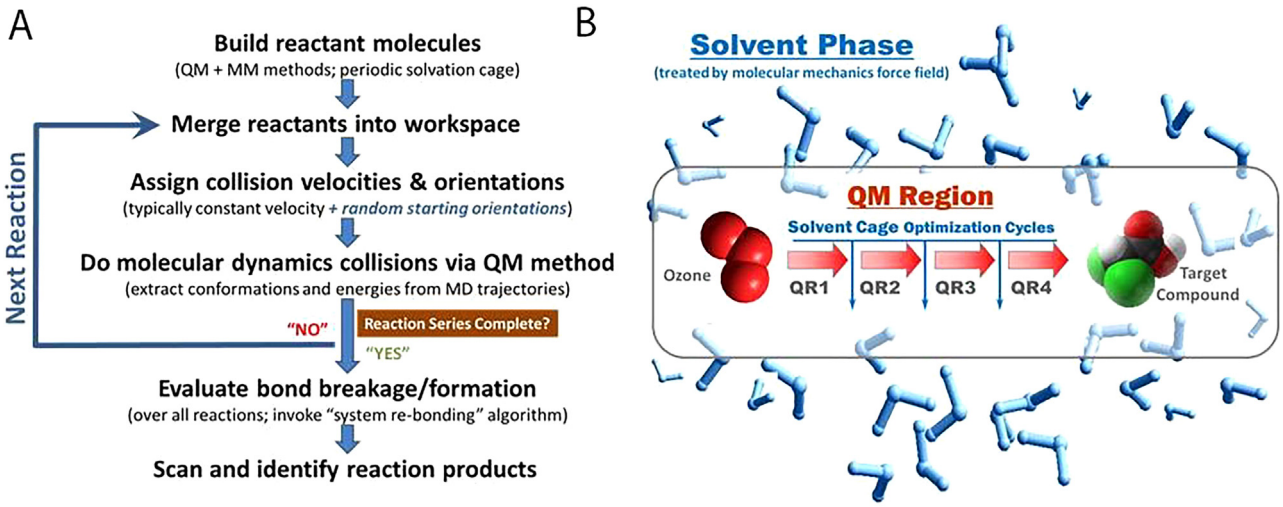


**Fig. 4.** A Outline of main steps involved in the SFMD reaction simulation algorithm. B: Diagram of the SFMD process.

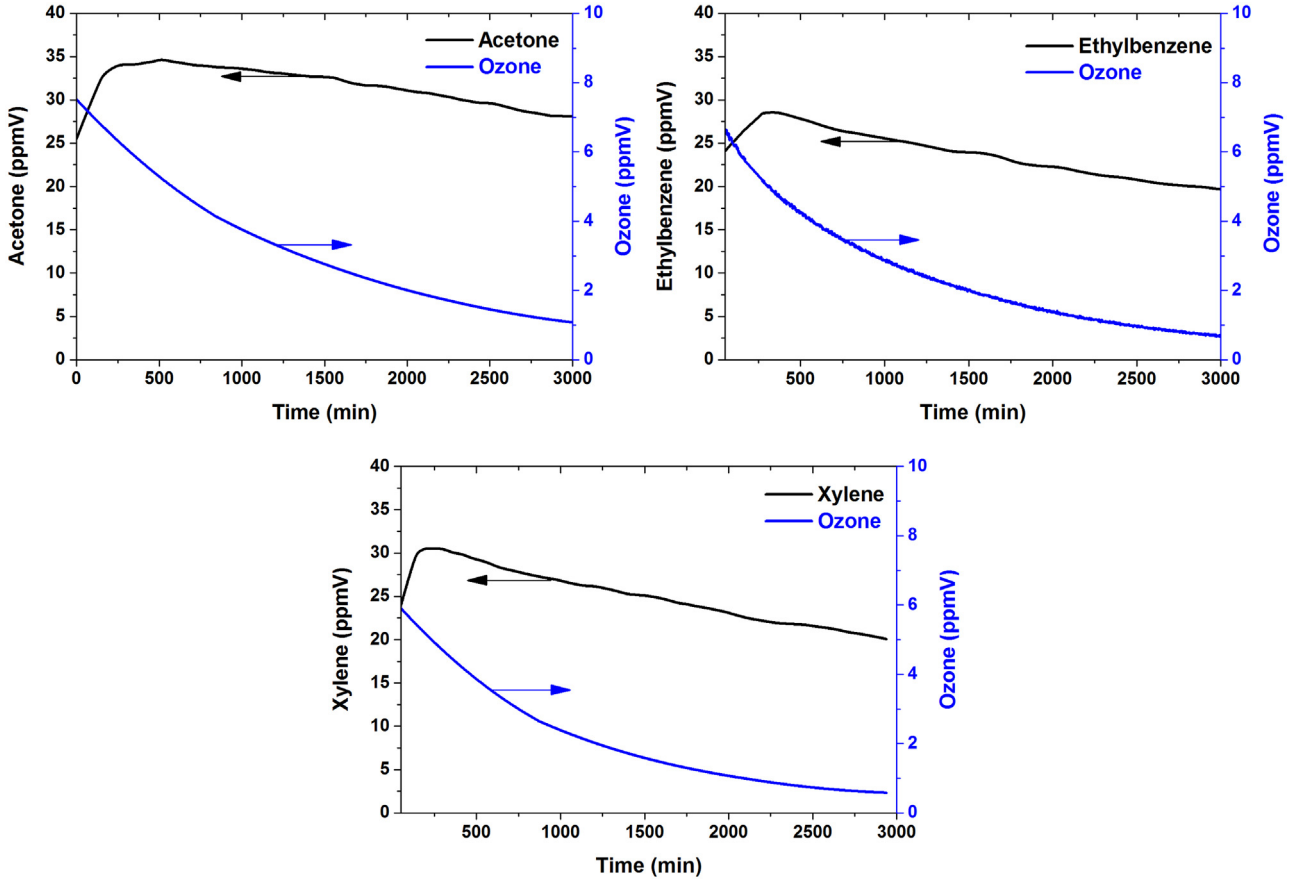


**Fig. 5.** Effect of ozone reaction with Acetone, Ethylbenzene and Xylene.

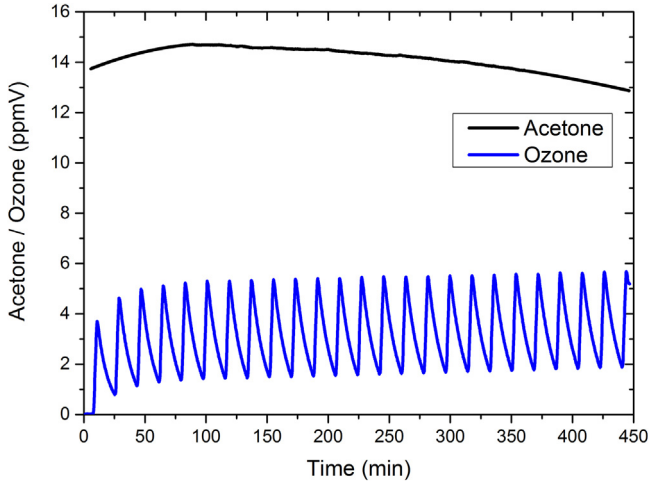


**Fig. 6.** Intermittent introduction of ozone and its reactivity with Acetone.

reaction between VOC and ozone were monitored for 50 h for each chemical. After 50 h of experimental duration, the concentration of Acetone was observed to reduce by 18.5%, Ethylbenzene was reduced by 25.4% while Xylene was reduced by 29.4%. It can be inferred from these results that Xylene readily reacts with ozone and degrades rapidly followed by Ethylbenzene and Acetone. It was also observed that no formaldehyde formation took place during the reaction between ozone and any of the pure chemicals.

It is apparent from Fig. 5 that Ozone reaction with Acetone is a slow process. In order to improve this reaction process, ozone was injected intermittently in to the chamber. Fig. 6 shows the effect of intermittent injection of ozone on reaction with Acetone. It was found that the concentration level of Acetone was reduced by 12.2% within 7.5 h. This reduction was about 4.4 times faster than that of single time injecting ozone in to the chamber. It is, therefore, clear that the intermittent introduction of small quantity of ozone enhances the reaction with VOCs.

### 3.2. Ozone/sabinene SFMD reaction simulations

A frequency histogram of the major product categories generated for the gas-phase reaction of sabinene with ozone is presented in Fig. 7A. These data were extracted from a total of 975 random bimolecular collisions (reaction trajectories) between ozone and the target compound. About one quarter of the collisions (25.9%) failed to result in any change to the parent compounds (i.e., ozone and sabinene). Such (failed) reactions were presumably unsuccessful because of unfavorable initial orientations of the reactants at the start of the collision trajectory (t = 0 ps). Approximately 86.4% of collisions resulted in single or double hydrogen abstraction with or without oxygen addition or substitution.

Oxygen addition or substitution reactions occurred in about 25.1% of the collisions, and ring opening occurred in about 9.7% of collisions. Only two instances of multi-oxygen addition were observed among the 975 collisions, although multi-oxygen products have been experimentally documented [18]. The addition of oxygen to either the main 5-member ring or the secondary (and more strained) 3-member ring was observed in about 18.7% of cases and a significant proportion of these instances resulted in ring scission, thereby creating linear aliphatic products. The formation of formaldehyde ($H_2C{=}O$) or formaldehyde-like precursor compounds was found in approximately 4.8% of collisions. Sabina-

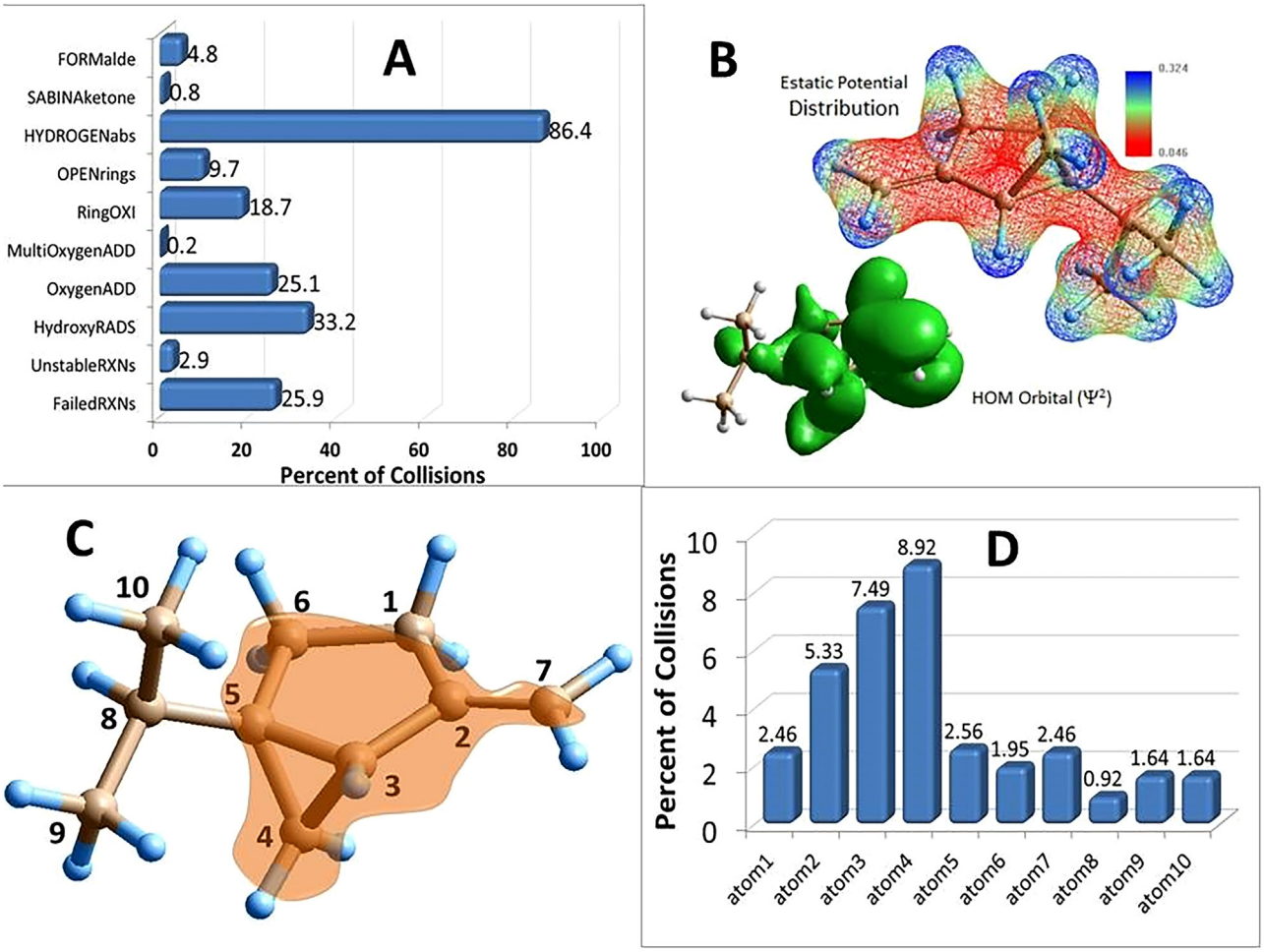


**Fig. 7.** A Frequency histogram based on 975 bimolecular collisions showing major product categories for the reaction of ozone with sabinene using the SFMD algorithm. B: Electrostatic charge distribution and electron orbital density in the highest occupied molecular (HOM) orbital of sabinene. C & D: Preferred sites of electrophilic oxygen addition or substitution on the 10 carbon centers of sabinene. Shaded region in panel C indicates region of molecule most susceptible to electrophilic attack.

ketone, which has been experimentally observed in gas-phase ozonation reactions [18], was formed in nearly 1% of the SFMD collisions.

Interestingly, nearly one-third of the collisions produced hydroxyl (OH) or peroxy radicals ($HO_2$, or $HO_3$). Peroxy radicals are somewhat elusive but have been recently experimentally observed in proton-irradiated water ice mixtures [19]. In addition, peroxy radicals are known to have played key roles in the chemistry of the troposphere where they have been implicated in atmospheric ozonation reactions [20]. Their presence in the current simulations suggests that they could play some role in secondary (i.e., second-generation) VOC transformations, although this was not further investigated due to excessive computational duration.

Based on the 975 bimolecular collisions that were carried out, the preferred sites of ozone oxygen addition or substitution on the sabinene molecule are shown in Fig. 7C and D. The most common sites of the initial ozone attack occurred at carbon atoms 1, 2, 3, 5, and 7, with reduced frequency of attack occurring at carbon atom centers 6, 8, 9, and 10. In general, ozonation (i.e., single or multi-oxygen addition or substitution) was most strongly associated with the two aliphatic rings and the C2=C7 double bond. These results are consonant with the electrostatic charge distribution for the sabinene molecule, as shown in Fig. 7B. Semi-empirical RM1 (and ab initio calculations – not shown) indicate that the primary electrostatic charge is mainly distributed over the aliphatic rings and the C2=C7 double bond region. Moreover, the $\Psi^2$ electron density of the highest occupied molecular (HOM) orbital was observed to be distributed across the aliphatic rings and the unsaturated double bond at carbon atoms 2 and 7 (Fig. 7B). Based on these calculations, electrophilic additions, substitutions and elimination reactions could be expected to occur most frequently at (or proximal to) the sabinene aliphatic rings and unsaturated bonds.

The formation of sabina-ketone is of particular relevance for this study since its formation has been previously demonstrated in gas-phase ozonation experiments reported by Yu et al. [18]. Thus, its occurrence among the ozone/sabinene reaction products lends support to the SFMD simulation protocol for the prediction of reaction outcomes. Results presented in Fig. 8 illustrate the mechanism by which sabina-ketone was formed in RXN#38 of the ozone/sabinene reaction series. The system potential energy (expressed in kcal/mol) and the separation distance (in Å) between the #1 oxygen atom of ozone and the terminal carbon atom of the C=$CH_2$ group in sabinene are plotted as a function of the elapsed time (in ps) for the reaction simulation. It is noteworthy that the ozone molecule reached its closest approach to the terminal C=$CH_2$ group at about 0.14 ps (see Fig. 8A and B). At about t = 0.167 ps, the ozone molecule had undergone homolytic dissociation forming molecular oxygen ($O_2$) and a single oxygen radical that immediately interacted with (and destabilized) the C=$CH_2$ *pi* bond. During the initial approach period, extending from t = 0 ps to about t = 0.105 ps, the system potential energy climbed steeply as the two molecules encountered Van der Waals and electrostatic repulsion

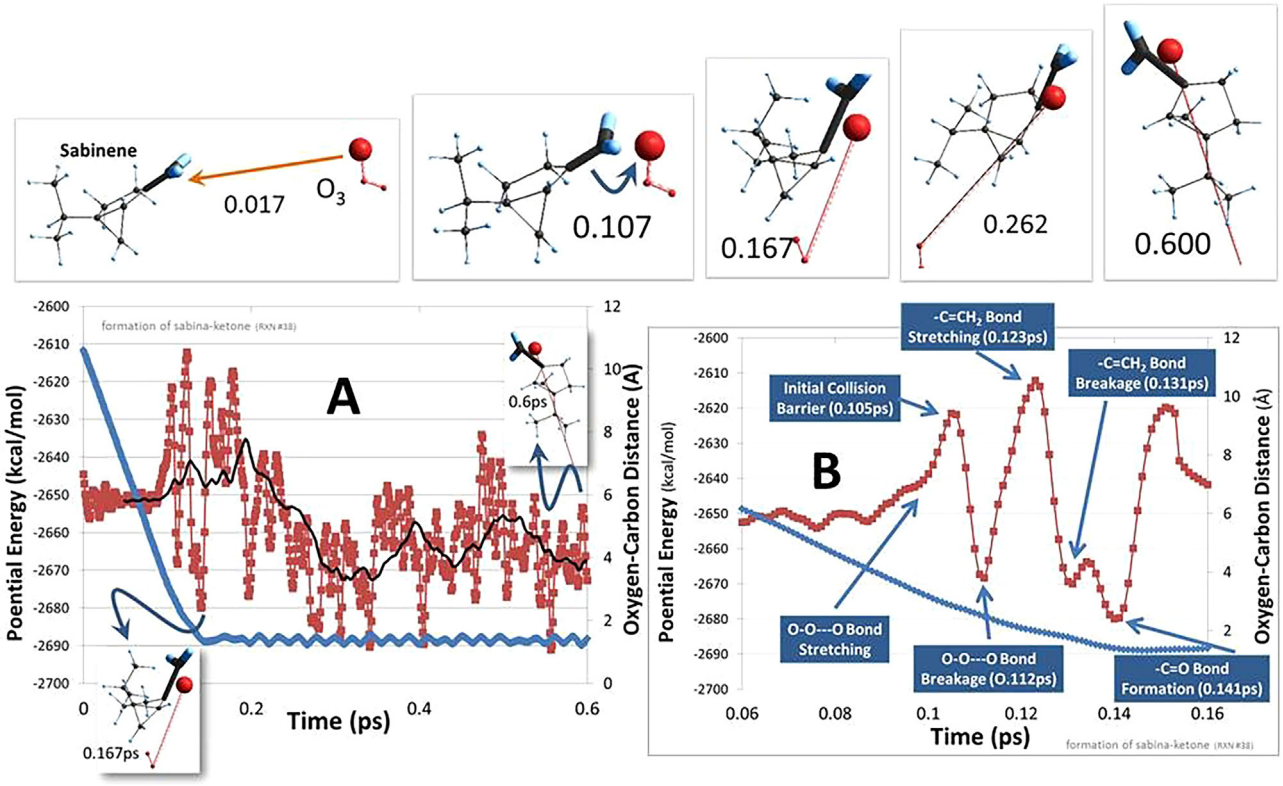


**Fig. 8.** Mechanism of formation of sabina-ketone in RXN#38 of the ozone/sabinene SFMD reaction series. Upper Panel: Selected frame captures (numbers are ps). (A): Brown = system potential (kcal/mol); Blue = separation distance between ozone oxygen atom #1 (large sphere) and the terminal $=CH_2$ carbon atom; Black = moving average (50) for system potential energy. Inset images = system (intermediate) conformations at denoted times. (B): Early period of RXN#38 trajectory from t = 0.06 ps to t = 0.16 ps. (For interpretation of the references to colour in this figure legend, the reader is referred to the web version of this article.)

barriers (see Fig. 8A and B). During this period, the hybridized O—O bond in ozone began to interact with the C=$CH_2$ double bond in sabinene. At t = 0.112 ps, the ozone O—O bond was completely dissociated, which was manifested as a distinct energy minimum at this time point. The O—O bond separation was coupled with the interaction of the released oxygen radical with the C=$CH_2$ double bond resulting in the destabilization and stretching of this bond, which reached a maximum strain energy at about t = 0.123 ps (see Fig. 8B). Dissociation of the C=$CH_2$ double bond was coupled with C=O ketone formation plus the release of a methylene ($CH_2$) fragment; events that resulted in two new energy minima observed at about t = 0.131 ps and t = 0.141 ps, respectively. Methylene (systematically named methylidene or dihydridocarbon), is a colorless gas that fluoresces in the mid-infrared range, and only persists in dilution or as an adduct.

The remaining energy fluctuations that are evident in Fig. 8A, following about t = 0.18 ps, were due to collision-induced kinetic/potential exchanges in the conformational space of the molecular system. They did not result in any further MO rearrangements (e.g., bond formation or dissociation events). It is apparent from inspection of Fig. 8A that the average potential energy of the molecular system was significantly lower following the oxygen-substitution/elimination reaction (i.e., after about t = 0.16 ps) compared to the unreacted parent compounds spanning the period from t = 0 ps to about t = 0.08 ps. This lowering in system potential is consistent with a thermodynamically favorable reaction path. A series of frame captures from RXN#38 are depicted in the upper panel of Fig. 8, which illustrate the progress and mechanism of the reaction sequence leading to formation of sabina-ketone.

A second reaction product that was of special interest was formaldehyde ($H_2C$=O), since it is a human carcinogen, highly volatile, and known to be off-gassed from synthetic textiles and a variety of building and insulation materials [21,22]. Moreover, it has been shown that formaldehyde may be generated *de novo* by the exposure of many types of building materials to ozone [21,22]. About 4.82% of the 975 ozone-sabinene collisions resulted in formaldehyde formation.

Data presented in Fig. 9 illustrate the mechanism of formaldehyde formation in RXN#73 of the ozone/sabinene SFMD series. In this reaction, ozone initially approaches carbon atom #4 of the strained 3-member propane ring of sabinene. This approach is manifested by a sharp increase in the strain potential of the system that reaches a maximum at t = 0.142 ps (see Fig. 9A and B). This potential maximum corresponds to Van der Waals and electrostatic repulsions that essentially constitute the primary activation energy for this reaction. During this period, the oxygen bonds of ozone undergo stretching and destabilization resulting in the homolytic dissociation and release of diatomic oxygen and a mono-oxygen radical at about t = 0.155 ps, which corresponds to a potential minimum (Fig. 9A and B). The oxygen cleavage is immediately coupled to electrophilic withdrawal from both ring bonds of carbon atom#4. The minor (propane) 3-member ring subsequently undergoes expansion and steric strain (as the carbon atom #4 bonds stretch and weaken) and finally dissociates completely at about t = 0.246 ps. This corresponds to a new potential energy minimum for the system. Individual frame captures show a number of intermediate conformations along the reaction path are presented in the upper panel of Fig. 9.

### 3.3. Ozone/benzene SFMD reaction simulations

Fig. 10 summarizes the results for the gas-phase SFMD simulation of the reaction of ozone with the aromatic compound benzene.

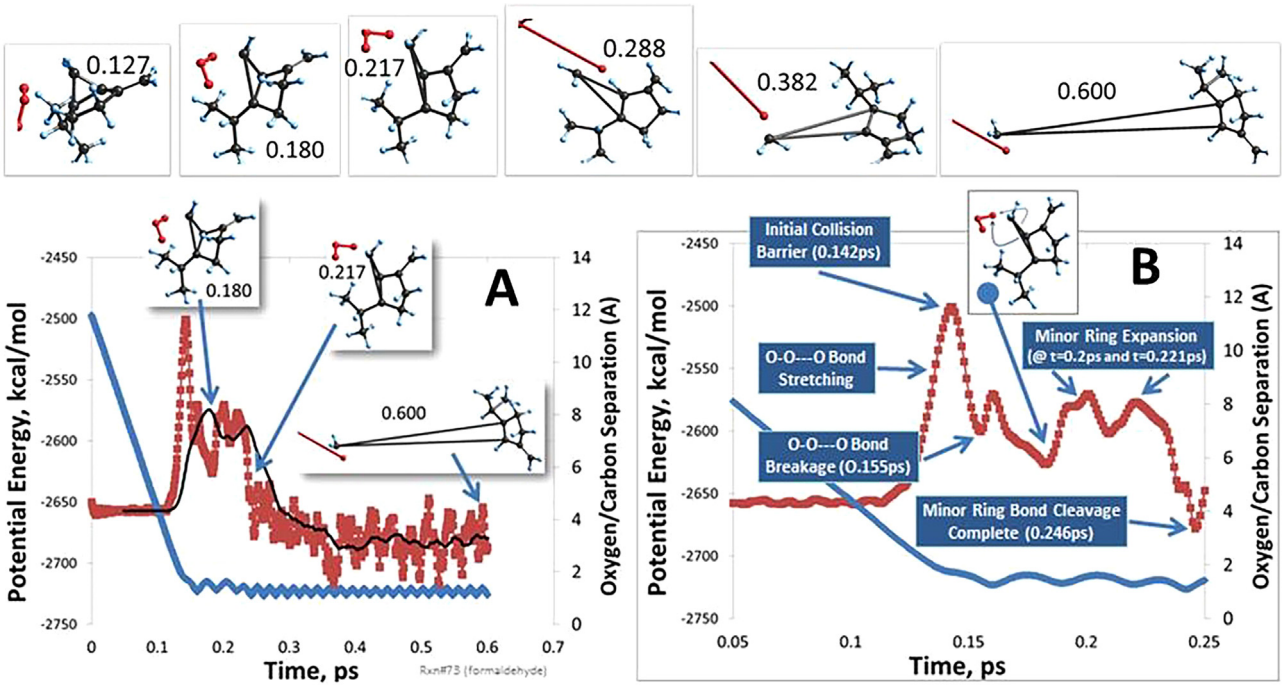


**Fig. 9.** Mechanism of formation of formaldehyde in RXN#73 of the ozone/sabinene series. Upper panel: Individual frame captures from the reaction trajectory. A: Entire RNX#73 collision trajectory showing system potential (Brown) and the separation distance (Blue) between the #1 oxygen atom of ozone and the #4 atom located at the apex of the propane minor ring of sabinene plotted as a function of the elapsed time. Solid black line = moving average of the potential energy. B: Region of trajectory spanning period from t = 0.05 ps to t = 0.25 ps. Text boxes denote bond rearrangement events. Symbols are same as in A. (For interpretation of the references to colour in this figure legend, the reader is referred to the web version of this article.)

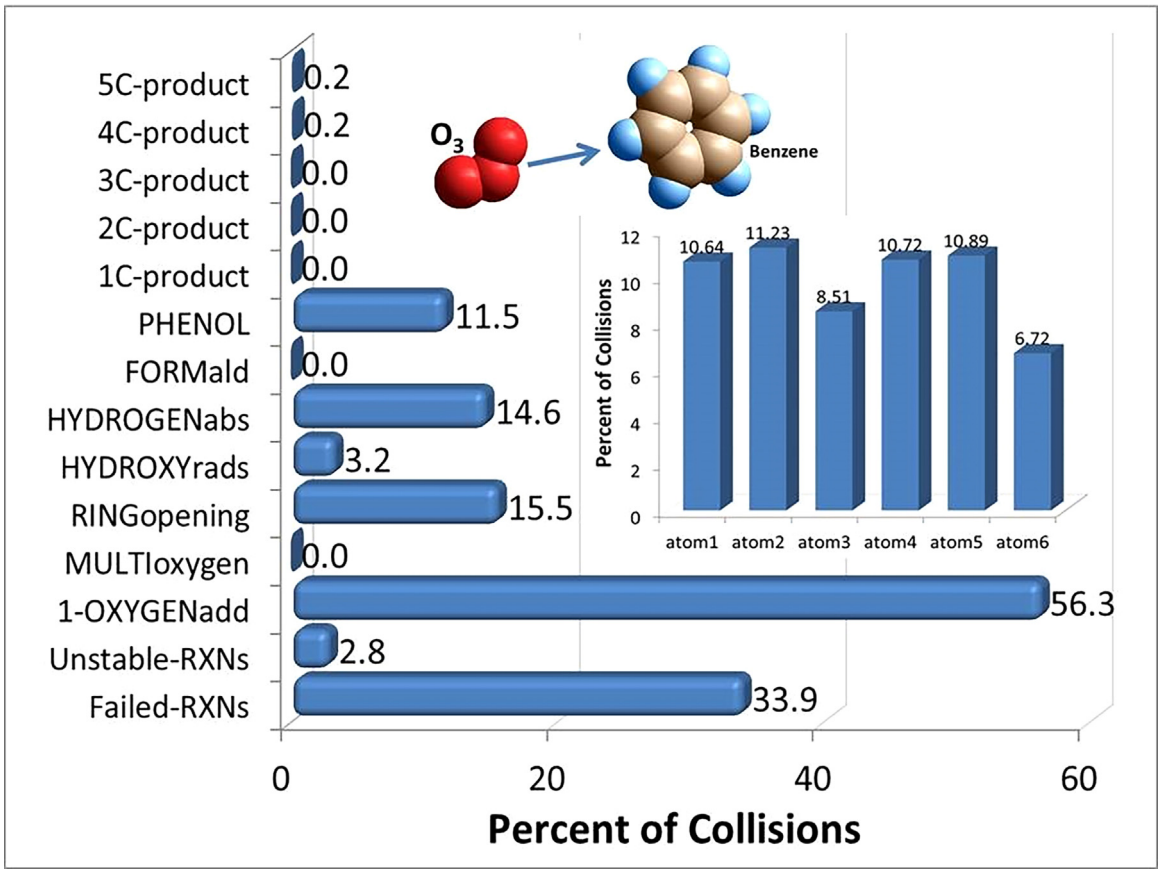


**Fig. 10.** Product distributions and atom center locations of electrophilic (oxygen radical) attack on the benzene ring in the SFMD simulation of the reaction of ozone with benzene.

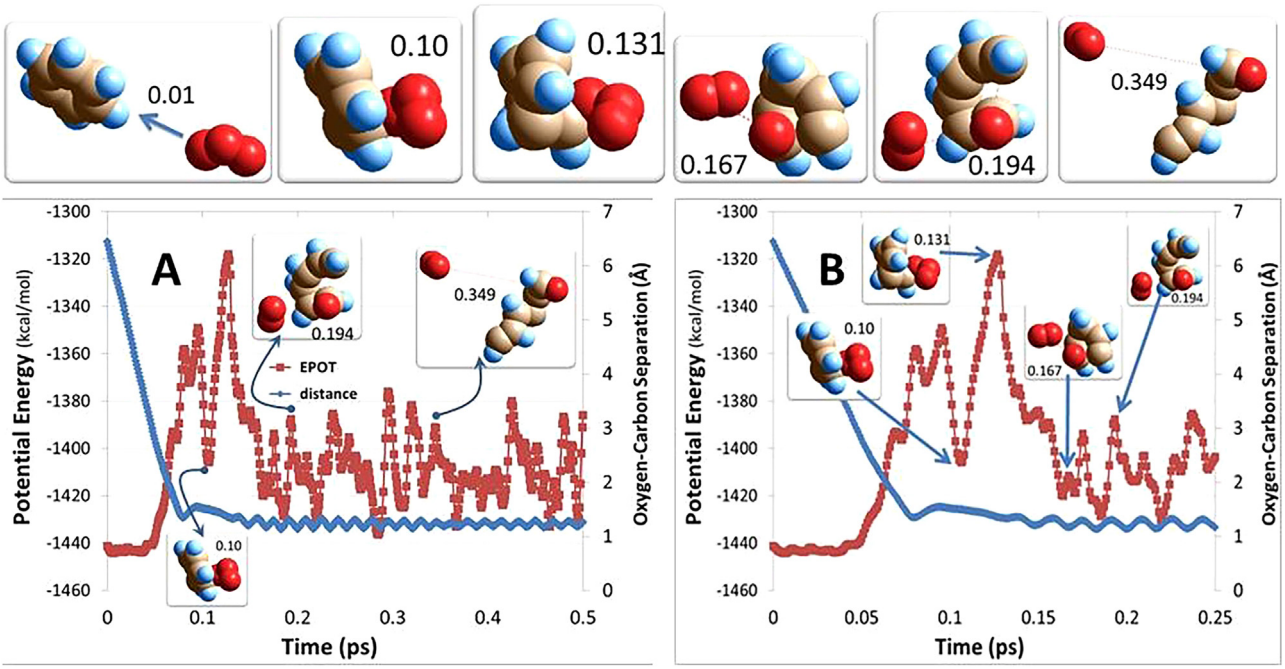


**Fig. 11.** Ozone/benzene RXN#36 that resulted in ring scission. Upper Row: Frame captures from RXN#36 trajectory showing progress of electrophilic oxygen-radical attack coupled with scission of the aromatic ring. A: Entire trajectory showing system potential and oxygen-carbon separation distance. Brown = potential energy; Blue = separation distance from ozone oxygen atom#1 and target carbon atom in benzene. B: Homolytic dissociation of the O—O bond in ozone yielding an oxygen radical which was completed by about t = 0.167 ps. (For interpretation of the references to colour in this figure legend, the reader is referred to the web version of this article.)

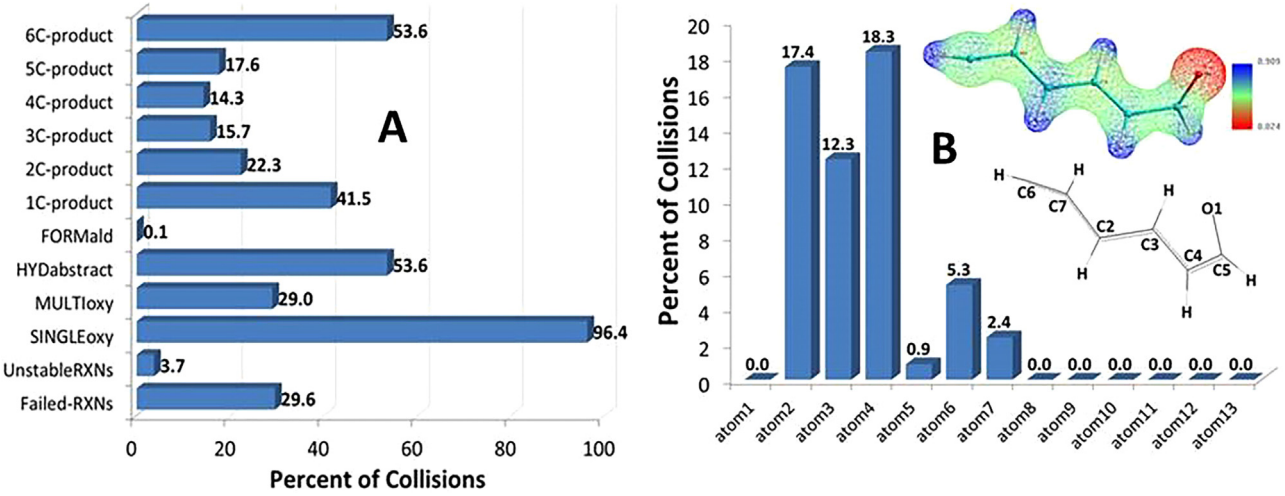


**Fig. 12.** (A) Major product categories for ozone reaction with the C6H6O open-ring intermediate produced in the ozone/benzene RXN#36, as described in the text. (B) Atom center preferences for electrophilic addition or substitution in the open-ring C6H6O target compound. Upper (color) inset shows the electrostatic charge distribution across the target compound (RM1, UHF calculation).

It is seen from this figure that about 96.2% of the 1198 bimolecular collisions analyzed resulted in single or double hydrogen abstraction from the benzene ring. A significant proportion of the hydrogen abstractions were coupled with oxygen additions (56.3%) and oxygen substitutions (11.5%). Approximately 15.5% of the collisions resulted in open-ring (i.e., linear chain) products. Unlike sabinene, no multi-oxygen addition products were observed in the first-generation benzene reactions. Similarly, no formaldehyde or formaldehyde-like precursor compounds were formed.

As shown in the inset graph of Fig. 10, there was no strong preference observed in the SFMD simulations for electrophilic oxygen addition or substitution reactions in benzene. This result is to be expected based on the isotropic symmetry of this compound. It is also noteworthy that the first-generation ozone/benzene reaction simulations did not result in significant fragmentation of the aromatic ring.

As indicated above, about 15.5% of the SFMD ozone/benzene reaction simulations yielded ring-scission products. Such open-ring intermediates are significant since they may be more susceptible to further (second-generation) electrophilic attack compared to the parent aromatic compound. The collision trajectory for one such "ring-scission" reaction, i.e., RXN#36 of the ozone/benzene series, is presented in Fig. 11. The progression of this reaction was similar to that observed for the electrophilic ozonation reactions described previously for sabinene. Initial collision took place between t = 0.075 ps and t = 0.127 ps (see Fig. 11A and B). This period was correlated with a homolytic dissociation of the O—O bond in ozone to yield molecular oxygen plus a "free" oxy-

gen radical. Radical formation was coupled with electrophilic attack on one of the ring carbon atoms. This sequence of events resulted in ring dissociation, which was completed by about t = 0.167 ps (see Fig. 11B). The system potential energy was somewhat higher after the ring opening than before, suggesting that the ring-scission product was likely an unstable intermediate compound. The open-ring product was identified as a $C_6H_6O$ carbocation with the SMILES notation of: C1C(=C)[C@@H]2C[C@@]2(C1)C(C)C. Additional frame captures illustrating the progression of events for this reaction simulation are presented in the upper panel of Fig. 11.

The open-ring compound from RXN#36 was subsequently employed as the target compound in a second-generation SFMD reaction series comprising 1400 bimolecular collisions to determine if it was more or less susceptible to ozone transformation compared to the parent benzene. The results of this SFMD simulation series are presented in Fig. 12A and B. Unlike ozonation of the parent benzene molecule, which did not produce many fragments, ozonation of the $C_6H_6O$ open-chain target compound resulted in the formation of many 1-, 2-, 3-, 4- and 5-carbon fragments. Among the fragments that were produced, 3- and 4-carbon fragments were least frequently observed (15.7% and 14.3%, respectively), whereas 1-carbon fragments were more common (41.5%). In spite of the higher occurrence of 1-carbon fragments, formaldehyde ($H_2C$=O) formation was marginal, found in only one instance of the 1400 collisions; a result consistent with our earlier experimental observation presented in Section 3.1. Multi-oxygen products (resulting from a single oxygen addition or substitution in the $C_6H_6O$ target compound) were observed in about 29% of the collisions and hydrogen abstractions occurred in about 53.6% of collisions. Based on the considerably broader diversity of the reaction products in this second-generation SFMD reaction series, it is concluded that the open-ring target compound was more susceptible to ozone-induced transformation compare to the parent benzene ring. Finally, the data presented in Fig. 12B indicates that most electrophilic (i.e., ozone oxygen-radical) attack occurred at carbon atom centers #2, #3 and #4. This pattern appears consistent with the presence of unsaturated (electron-rich) or hybridized carbon–carbon bonds associated with these atomic loci.

## 4. Conclusions

In this study, both experimental and simulation of gas-phase ozone reactions with VOCs were carried out. From experiments, it was found that ozone reacts with pure VOC components and effectively reduces its concentration. Reaction of ozone with Xylene is faster followed by Ethylbenzene and finally Acetone in a ranking order. When ozone was introduced intermittently, the reaction with Acetone was enhanced by about 4.4 times. In order to understand the specific intermediates and stable end products, molecular dynamic (MD) simulations were carried out in this work and key results revealed that:

(1) In first and second generation SFMD simulations, ozone reacted with volatile aromatic hydrocarbons (e.g., benzene), C6 straight-chain benzene derivatives, and alicyclic monoterpene VOCs, such as sabinene, to form a wide range of transformation byproducts;
(2) Ozone transformations of the target VOCs occurred mainly by electrophilic addition or substitution/elimination mechanisms that were often coupled to hydrogen abstraction, ring-scission processes, and release of short-chain carbon fragments (e.g., the methylene compound:$CH_2$);
(3) Compared to the parent aromatic compound benzene, a second-generation $C_6H_6O$ open-ring product (derived from an initial first-generation ozone/benzene reaction) was found to be much more susceptible to fragmentation by ozone, producing a series of C1 through C5 fragments. Such fragments were typically unstable carbocations that could be expected to undergo further transformations spontaneously or by subsequent ozone exposure;
(4) Formation of formaldehyde ($H_2C$=O) was observed in reactions of ozone with either benzene or sabinene, although substantially greater levels of formaldehyde were produced by the monoterpene. Moreover, formaldehyde formation in the ozone/benzene reactions was only observed when the second-generation $C_6H_6O$ open-ring product was used as the target compound; and
(5) Ozone/sabinene reactions resulted in the formation of sabina-ketone in a significant fraction (0.8%) of bimolecular collisions. Sabina-ketone has been experimentally demonstrated as an ozonation product in gas-phase reactions [18]. This observation lends validity to the SFMD algorithm for the prediction of VOC oxidation products.

## Acknowledgement

The authors gratefully acknowledge the generous funding from the National Research Foundation (NRF) Singapore under the Energy Innovation Research Programme (EIRP) Funding Scheme (R-265-000-515-279) managed on behalf by Building and Construction Authority (BCA).

## References

[1] L.A. Wallace, Human exposure to volatile organic pollutants: implications for indoor air studies, Annu. Rev. Energy Environ. 26 (2001) 269–301.
[2] M. Kampa, E. Castanas, Human health effects of air pollution, Environ. Pollut. 151 (2008) 362–367, http://dx.doi.org/10.1016/j.envpol.2007.06.012.
[3] D.A. Sarigiannis, S.P. Karakitsios, A. Gotti, I.L. Liakos, A. Katsoyiannis, Exposure to major volatile organic compounds and carbonyls in European indoor environments and associated health risk, Environ. Int. 37 (2011) 743–765, http://dx.doi.org/10.1016/j.envint.2011.01.005.
[4] W.H. Organization, Air Quality Guidelines for Europe, 2000.
[5] ASHRAE Standard 62-1999, Ventilation for Acceptable Indoor Air Quality, Am. Soc. Heat. Refrig. Air-Conditioning Eng. (1999).
[6] K. Cheong, K. Chong, Development and application of an indoor air quality audit to an air-conditioned building in Singapore, Build. Environ. 36 (2001) 181–188, http://dx.doi.org/10.1016/S0360-1323(99)00064-5.
[7] S. Ginestet, D. Marchio, Control tuning of a simplified VAV system: methodology and impact on energy consumption and IAQ, Energy Build. 42 (2010) 1205–1214, http://dx.doi.org/10.1016/j.enbuild.2010.02.011.
[8] K.J. Chua, S.K. Chou, W.M. Yang, J. Yan, Achieving better energy-efficient air conditioning—a review of technologies and strategies, Appl. Energy 104 (2013) 87–104, http://dx.doi.org/10.1016/j.apenergy.2012.10.037.
[9] F.I. Khan, A. Kr Ghoshal, Removal of volatile organic compounds from polluted air, J. Loss Prev. Process Ind. 13 (2000) 527–545, http://dx.doi.org/10.1016/S0950-4230(00)00007-3.
[10] J.M. Estrada, O.I. Bernal, M.C. Flickinger, R. Muñoz, M.A. Deshusses, Biocatalytic coatings for air pollution control: a proof of concept study on VOC biodegradation, Biotechnol. Bioeng. 112 (2015) 263–271.
[11] M.F. Boeniger, Use of ozone generating devices to improve indoor air quality, Am. Ind. Hyg. Assoc. J. 56 (1995) 590–598, http://dx.doi.org/10.1080/15428119591016827.
[12] C.W. Kwong, C.Y.H. Chao, K.S. Hui, M.P. Wan, Removal of VOCs from indoor environment by ozonation over different porous materials, Atmos. Environ. 42 (2008) 2300–2311, http://dx.doi.org/10.1016/j.atmosenv.2007.12.030.
[13] A. Berenjian, N. Chan, H.J. Malmiri, Volatile organic compounds removal methods: a review, Am. J. Biochem. Biotechnol. 8 (2012) 220.
[14] A. Hassani, M. Keyvanfar, A. Hassani, Volatile organic compounds (VOCs) removal of polluted air streams using ozone in the presence of porous silica bed, Aust. J. Basic Appl. Sci. 5 (2011).
[15] R. Munter, Advanced oxidation processes–current status and prospects, Proc. Est. Acad. Sci. Chem. 50 (2001) 59–80.
[16] C.J. Weschler, Ozone in indoor environments: concentration and chemistry, Indoor Air 10 (2000) 269–288.
[17] G.B. Rocha, R.O. Freire, A.M. Simas, J.J.P. Stewart, RM1: a reparameterization of AM1 for H, C, N, O, P, S, F, Cl, Br, and I, J. Comput. Chem. 27 (2006) 1101–1111.
[18] J. Yu, D.R. Cocker III, R.J. Griffin, R.C. Flagan, J.H. Seinfeld, Gas-phase ozone oxidation of monoterpenes: gaseous and particulate products, J. Atmos. Chem. 34 (1999) 207–258.
[19] P.D. Cooper, M.H. Moore, R.L. Hudson, Infrared detection of $HO_2$ and $HO_3$ radicals in water ice, J. Phys. Chem. A 110 (2006) 7985–7988.

[20] P.S. Monks, Gas-phase radical chemistry in the troposphere, Chem. Soc. Rev. 34 (2005) 376–395.
[21] N. Kagi, S. Fujii, H. Tamura, N. Namiki, Secondary VOC emissions from flooring material surfaces exposed to ozone or UV irradiation, Build. Environ. 44 (2009) 1199–1205.
[22] M. Nicolas, O. Ramalho, F. Maupetit, Reactions between ozone and building products: impact on primary and secondary emissions, Atmos. Environ. 41 (2007) 3129–3138.